

## A metal-lustrous porphyrin foil

Mitsuhiko Morisue,<sup>\*†</sup> Yuki Hoshino,<sup>†</sup> Masaki Shimizu,<sup>†</sup> Shogo Tomita,<sup>‡</sup> Sono Sasaki,<sup>‡</sup> Shinichi Sakurai,<sup>‡</sup> Takaaki Hikima,<sup>#</sup> Ayaka Kawamura,<sup>§</sup> Michinari Kohri,<sup>§</sup> Jun Matsui,<sup>¶</sup> and Takeshi Yamao<sup>€</sup>

<sup>†</sup>Faculty of Molecular Chemistry and Engineering, and <sup>‡</sup>Faculty of Fiber Science and Engineering, Kyoto Institute of Technology, Matsugasaki, Sakyo-ku, Kyoto 606-8585, Japan.

<sup>#</sup>RIKEN SPring-8 Center, 1-1-1, Kouto, Sayo-cho, Sayo-gun, Hyogo 679-5148, Japan.

<sup>§</sup>Division of Applied Chemistry and Biotechnology, Graduate School of Engineering, Chiba University, 1-33 Yayoi-cho, Inage-ku, Chiba 263-8522, Japan

<sup>¶</sup>Department of Material and Biological Chemistry, Faculty of Science, Yamagata University, Kojirakawa-cho, Yamagata, 990-8560, Japan.

<sup>€</sup>Faculty of Materials Science and Engineering, Kyoto Institute of Technology, Matsugasaki, Sakyo-ku, Kyoto 606-8585, Japan.

### 1. General Method

NMR spectra were recorded on Bruker AV-300. Matrix-assisted laser-dissociation ionization time-of-flight (MALDI-TOF) mass spectra were recorded on mass spectrometer (Bruker, Autoflex Speed). UV/vis absorption spectra were recorded on a spectrophotometer (Shimadzu, UV-1800) equipped with a Peltier thermoelectric temperature controlling unit (Shimadzu, TCC-240A). The thickness of porphyrin foil was measured by a thickness gauge. Absolute reflection spectrum was performed by JASCO MSV-370 (0° of incident and reflection angles for Fig 2A), and reflection angle-dependence was conducted by JASCO ARSV-732 equipped with V-650/B13861150 (5° of incident angle ( $\theta$ ) and varying reflection angles  $\phi$  for Fig S1). X-ray fluorescence (XRF) was performed by Rigaku ZSX primus II. Spectrometric ellipsometry was recorded by Otsuka Electronics FE-5000S. The glass transition temperature ( $T_g$ ) was observed under nitrogen stream by differential scanning calorimeter (Shimadzu, DSC-60Plus). Analytical size-exclusion chromatography was performed by a PU-2086 Plus (JASCO) equipped with columns of Shodex GPC LF-804  $\times$  2 in a column oven (JASCO, 860-CO) with THF as the eluent, monitored by a UV detector (JASCO, UV-1570) and a RI detector (Shodex, RI-101).

Fig. S1. Schematic representation of the colour wheel.

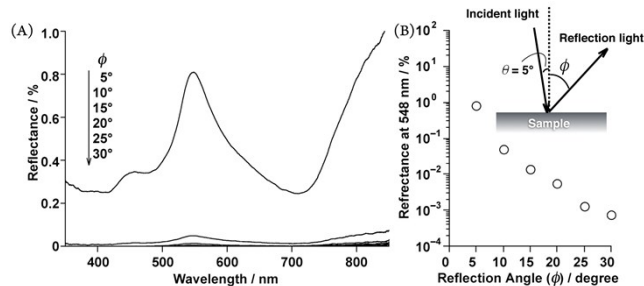
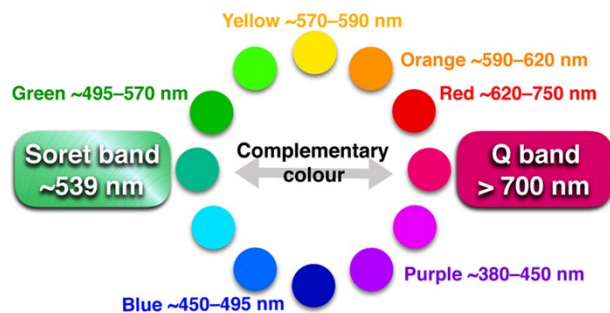
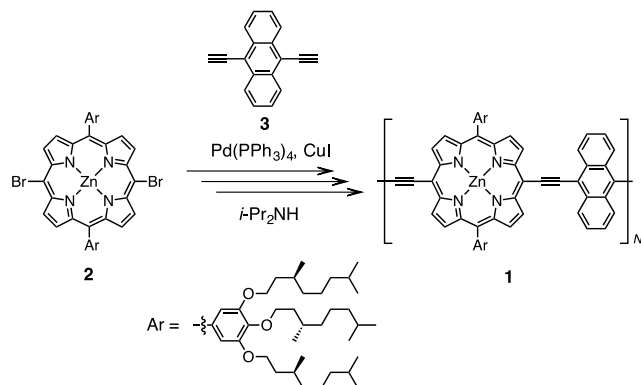


Fig. S2. Reflection angle-dependence in reflection spectra of the porphyrin foil, observed at a constant incident angle of 5° (A), and the plot of reflectance at 548 nm (B). Inset shows the configuration of experimental set-up.



## 2. Synthesis of 1.

Porphyrin **1** was synthesized via Sonogashira–Hagihara coupling reaction of porphyrin **2** and 9,10-bis(ethynyl)anthracene **3** using a Schlenk technique.<sup>S1,S2</sup> A solution of **2** (0.30 g, 0.19 mmol) in *i*-Pr<sub>2</sub>NH (5 mL) in a Schlenk tube was degassed by freeze-pump-thaw cycles. To the solution, a solution of **3** (42 mg, 0.19 mmol) in THF (5 mL), Pd(PPh<sub>3</sub>)<sub>4</sub> (10 mg, 8.6 μmol), and CuI (3 mg, 16 μmol), which was separately degassed by freeze-pump-thaw cycles, was added. The mixture was stirred at 70 °C for 4 days. The reaction mixture was diluted with chloroform/pyridine mixture, and then successively washed with water and brine. The organic layer was dried over anhydrous sodium sulfate. The residue dissolved in chloroform with 10% pyridine was repetitively reprecipitated from methanol and *n*-hexane. The solution of the product **1** in chloroform with 10% pyridine placed in a round-bottom flask was dried using a rotary evaporator, and then the product on the wall of the flask peeled off with the addition of methanol. Then, a “porphyrin foil” of **1** (0.3 g) was obtained in a 96% yield. An alternating porphyrin–anthracene sequence was identified based on 1:1 content of porphyrin–anthracene as well as no multiplied signals of them in pyridine-*d*<sub>5</sub> in <sup>1</sup>H and <sup>13</sup>C NMR spectra. The Sonogashira–Hagihara coupling reaction exclusively proceeded to provide **1**. <sup>1</sup>H NMR (300 MHz, CDCl<sub>3</sub> with 5% pyridine-*d*<sub>5</sub>): δ 10.11 (brs, 4H; porphyrin-β), 9.56 (brs, 4H; anthracene), 9.18 (brs, 4H; porphyrin-β), 8.00 (brs, 4H, 4H; anthracene), 7.54 (s, 4H; Ar), 4.41–4.24 (brm, 12H, -O-CH<sub>2</sub>-), 2.35–0.84 ppm (m, 114H; alkyl). <sup>13</sup>C NMR (75 MHz, CDCl<sub>3</sub> with 5% pyridine-*d*<sub>5</sub>): δ 152.4, 151.3, 150.3, 138.1, 133.3, 127.4, 123.7, 114.5, 101.6, 72.1, 67.8, 39.5, 39.3, 37.7, 37.5, 36.7, 30.0, 28.1, 28.0, 24.9, 24.8, 22.8, 22.7, 22.6, 19.9, 19.8, 19.2 ppm. Molecular weight of **1** was determined to be *M*<sub>n</sub> = 54,000 and *M*<sub>w</sub>/*M*<sub>n</sub> = 4.2 using polystyrene as the standard (Fig. S3). The XRF measurement found no bromine terminal.



Scheme 1. Synthesis of polymer **1**.

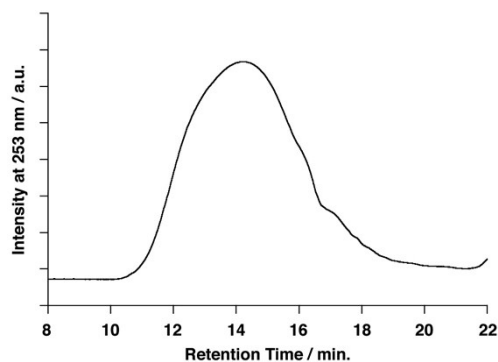


Fig. S3. SEC profile of **1** with THF as the eluent.

## 3. Static contact angle measurements.<sup>S3</sup>

The static contact angle ( $\theta$ ) of H<sub>2</sub>O and CH<sub>2</sub>I<sub>2</sub> was observed. Based on the Young equation, the surface free energy ( $\gamma$ ) is the sum of a dispersion force component ( $\gamma^d$ ) and a hydrogen bonding (dipole–dipole interaction) component ( $\gamma^h$ ), *i.e.*,  $\gamma = \gamma^d + \gamma^h$ . Then, simultaneous Owens equations of  $\theta$  for H<sub>2</sub>O and CH<sub>2</sub>I<sub>2</sub> give  $\gamma^d$  and  $\gamma^h$ , and therefore  $\gamma$ . The Owens equation defines the surface free energy of liquid ( $\gamma_l$ ) as:  $\gamma_l(1 + \cos\theta) = 2(\gamma_{\text{solid}}^d \gamma_{\text{liq}}^d)^{1/2} + 2(\gamma_{\text{solid}}^h \gamma_{\text{liq}}^h)^{1/2}$ , wherein  $\gamma_{\text{liq}}^d = 21.8$  (H<sub>2</sub>O) and 49.5 mN·m<sup>-1</sup> (CH<sub>2</sub>I<sub>2</sub>), and  $\gamma_{\text{liq}}^h = 51$  (H<sub>2</sub>O) and 1.3 mN·m<sup>-1</sup> (CH<sub>2</sub>I<sub>2</sub>). Accordingly,  $\gamma^d$  and  $\gamma^h$  of the porphyrin foil were estimated to be 35.5 and 0.40 mN·m<sup>-1</sup>, respectively. Therefore, the  $\gamma$  value was determined to be 35.9 mN·m<sup>-1</sup>.

## 4. Synchrotron X-ray scattering measurements.

The wide-angle X-ray scattering (WAXS) and ultra-small angle X-ray scattering (USAXS) experiments of the porphyrin foil were performed using synchrotron radiation at the BL45XU and BL19B2 beamline, respectively, in SPring-8 (RIKEN SPring-8 Centre Hyogo, Japan). The WAXS experiment were carried out using the combination of an image intensifier and a CMOS camera (Hamamatsu Photonics K. K.) or a PILATUS 300K-W (Dectris Ltd.) at 308.6 mm of the sample-to-detector distance. The USAXS experiment were carried out using the combination of an image intensifier and a CMOS camera (Hamamatsu Photonics K. K.) or a PILATUS 300K-W (Dectris Ltd.) at 40 m of the sample-to-detector distance.

## 5. Field-effect transistor experiments

Field-effect transistor experiments were performed in vacuum ( $\sim 10^{-3}$  Pa) using two source meters (Keithley 2400). A toluene solution of **1** was cast on a microgap Au electrodes (channel length: 10 μm, channel width: 2 mm, height: 100 nm), wherein the Au electrodes were fabricated

on surface-oxidized Si substrates as the source and drain contacts.

The hole mobility,  $\mu$ , was determined in the linear region based on the following equation.

$$I_D = (W/L)\mu C_i(V_G - V_{th})V_D$$

wherein  $I_D$  is the drain current,  $L$  ( $= 1.0 \times 10^{-3}$  cm) and  $W$  ( $= 0.2$  cm) are the channel length and width, respectively,  $C_i$  is the insulator capacitance per unit area ( $C_i = \epsilon_i \epsilon_0/D$ , where  $\epsilon_0$  is the permittivity of vacuum  $= 8.854 \times 10^{-12}$  F  $\text{cm}^{-1}$ ,  $\epsilon_i$  is the relative permittivity of  $\text{SiO}_2 = 3.9$ ,  $D$  is the thickness of  $\text{SiO}_2$  layer  $= 300$  nm),  $V_G$ ,  $V_{th}$ , and  $V_D$  are the gate voltage, threshold voltage, and drain voltage, respectively. The average hole mobility was roughly estimated as  $\mu = (4.0 \pm 1.4) \times 10^{-6}$   $\text{cm}^2 \text{V}^{-1} \text{s}^{-1}$  under the conditions, where gate voltage was applied from  $-10$  to  $-50$  V (Fig. S4). The result was moderate, comparing with the reported values,<sup>S4</sup> considering the fact that we did not optimize the experimental conditions at this moment.

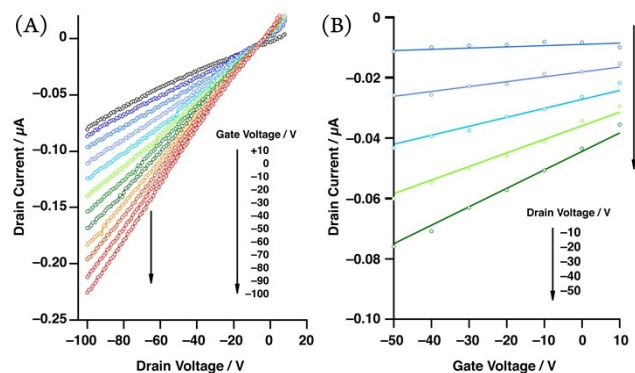


**Fig. S4.** (A) Drain current–drain voltage ( $I_D$ – $V_D$ ) characteristics of **1** as a function of the gate voltage ( $V_G$ ). (B) Drain current–gate voltage ( $I_D$ – $V_G$ ) characteristics of **1** as a function of the drain voltage ( $V_D$ ) in the linear region. (Electrode:  $L = 10$   $\mu\text{m}$  and  $W = 2$  mm).

## References

- [S1] M. Morisue, Y. Hoshino, K. Shimizu, M. Shimizu, Y. Kuroda, *Chem. Sci.* 2015, **6**, 6199–6206.
- [S2] Y.-P. Ou, C. Jiang, D. Wu, J. Xia, J. Yin, S. Jin, G.-A. Yu, S. H. Liu, *Organometallics* 2011, **30**, 5763–5770.
- [S3] D. K. Owens, *J. App. Polym. Sci.* 1969, **13**, 1741–1747.
- [S4] X. Huang, C. Zhu, S. Zhang, W. Li, Y. Guo, X. Zhang, Y. Liu, Z. Bo, *Macromolecules* 2008, **41**, 6895–6902.

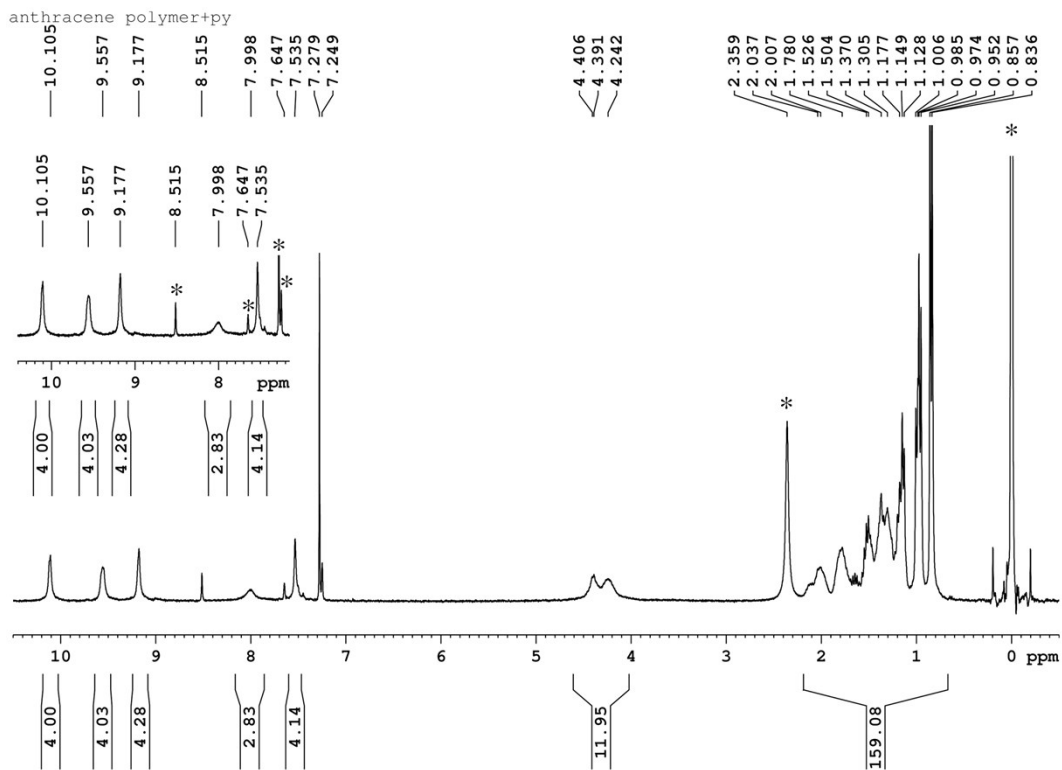


Fig. S6.  $^1\text{H}$  NMR (300 MHz,  $\text{CDCl}_3$  with 5% pyridine- $d_5$ ) of **1**. Asterisk indicates residual solvent and water.

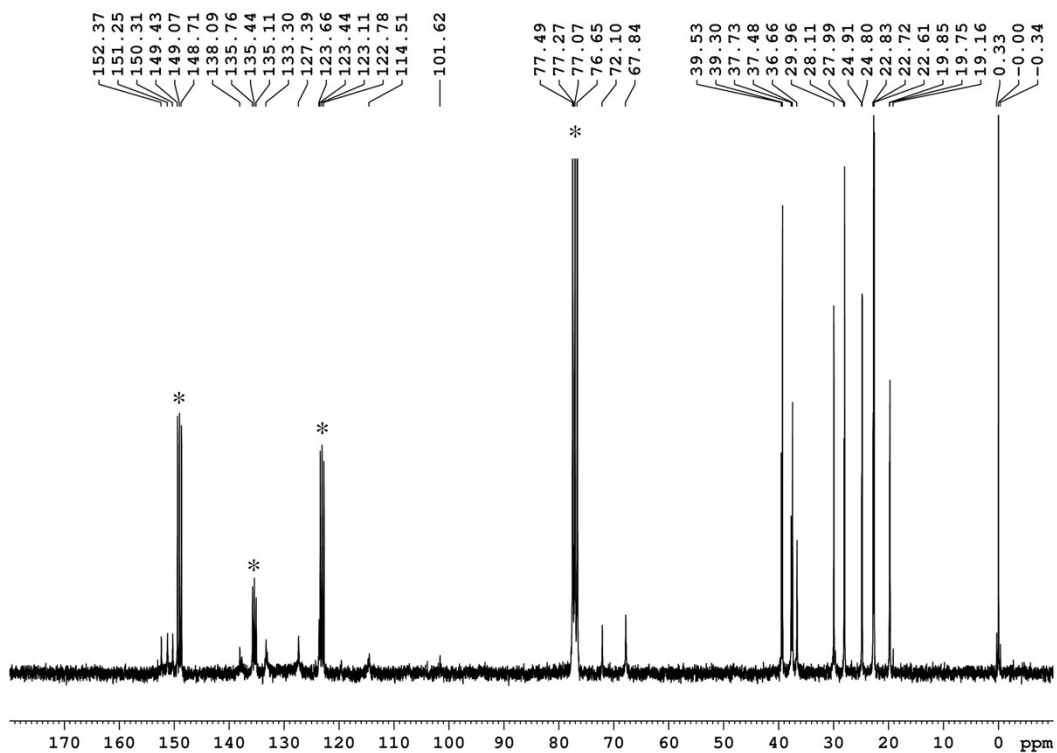


Fig. S7.  $^{13}\text{C}$  NMR (75 MHz,  $\text{CDCl}_3$  with 5% pyridine- $d_5$ ) of **1**. Asterisk indicates solvent.